New Inverting Modified CUK Converter Configurations with Switched Inductor (MCC_{SI}) for High-Voltage/Low-Current Renewable Applications

Pandav Kiran Maroti*, Sanjeevikumar Padmanaban**, Mahajan Sagar Bhaskar***,
Frede Blaabjerg†, Patrick Wheeler††
*DEPT. OF ELECTRICAL & ELECTRONICS ENGG., MARATHWADA INSTITUTE OF TECHNOLOGY, AURANGABAD, INDIA.
**DEPT. OF ENERGY TECHNOLOGY, AALBORG UNIVERSITY, ESBJERG, DENMARK.
***DEPT. OF ELECTRICAL ENGG., QATAR UNIVERSITY, DOHA, QATAR.
†CENTER OF RELIABLE POWER ELECTRONICS (CORPE), DEPT. OF ENERGY TECHNOLOGY, AALBORG UNIVERSITY, AALBORG, DENMARK.
††POWER ELECTRONICS, MACHINES & CONTROL GROUP (PEMC), DEPT. OF ELECTRICAL & ELECTRONICS ENGG., NOTTINGHAM UNIVERSITY, NOTTINGHAM, UNITED KINGDOM.
E-Mail: *kiranpandav88@yahoo.co.in,
**san@et.aau.dk,
***sagar25.mahajan@gmail.com,
†fbl@et.aau.dk,
††pat.wheeler@nottingham.ac.uk

Keywords

«CUK Converter», «High Voltage», «Low Current», «DC-DC Converter», «Renewable Energy».

Abstract

Inverting Modified CUK Converter with Switched Inductor (MCC_{SI}) configurations are articulated in the paper for high-voltage and low-current renewable energy applications. Based on the Switched Inductor (SI) position in MCC converter, four new modified CUK converter configurations are proposed as MCC_{SI}-XLL, MCC_{SI}-LYL, MCC_{SI}-LLZ and MCC_{SI}-XYZ. The mathematical analysis and comparison is shown in terms of the voltage conversion ratio, number of active and reactive components. The mode of operation of MCC_{SI}-XLL configuration is discussed to understand the working concept of MCC_{SI} configurations. The striking features of the proposed configurations are discussed in details. Operation of the proposed converter is verified by simulation in MatLab R2016a.

Introduction

From the last decades, researchers attract more towards renewable energy sources to fulfill the present and future demand of electrical energy due to free of cost, availability, plentiful in nature and pollution free [1]-[3]. The photovoltaic and wind technologies are more popular and developing with higher rate compared to other renewable energy sources. It is compulsory to boost the terminal voltage of photovoltaic source because low voltage is generated from the photovoltaic cells [4]-[5]. Thus, DC-DC power converter plays a vital role in the implementation of a photovoltaic system. Based on the contact of input and output terminals, DC-DC converters are classified into two categories as isolated and non-isolated [6]. Isolated converter requires transformer and coupled inductors which makes converter bulky and heavy. The efficiency of the isolated converter decreases due to a leakage inductor of transformers and Electromagnetic Interference (EMI). Non isolated converters are generally low weighted and small in size compared to isolated converter due to absence of transformer [7]-[8]. The boost and buck-boost converters are conventional DC-DC converter designed by using single switch, diode and singe inductor. Boost converter has a continuous current at input side with non-inverting voltage conversion ratio whereas buck-boost converter have discontinuous current at input side with

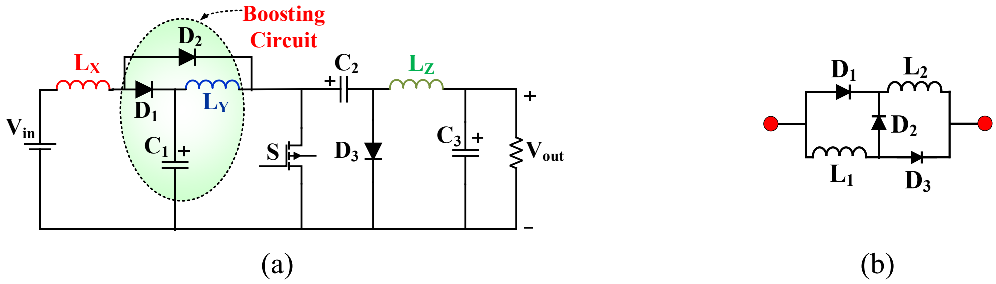

Fig. 1: (a) Modified CUK converter and (b) SI module

inverting voltage conversion ratio [9]. CUK converter is derived by combining the feature of buck and boost converter. CUK converter has continuous input and output current with inverting output voltage conversion ratio. Boost, Buck-Boost and CUK converter is not a feasible solution to achieve a high voltage conversion ratio [10].

The cascaded boost converter has the capability to generate high voltage, but the efficiency of these converters is less due to several control switches. Recently, various DC-DC converters are addressed to achieve a high voltage conversion ratio by modifying the conventional converters [11]-[12]. Multilevel converters are proposed by combining the feature of voltage multiplier circuitry with conventional converters to achieve a high voltage conversion ratio. In [13], inverting 2Nx converter is proposed to achieve N time's voltage conversion ratio compared to conventional boost converter where N is the number of levels of multiplier. Although the multilevel converters are provide high voltage conversion ratio, but requires more number of diodes and capacitor. Switched Inductor (SI), Switched Capacitor (SC) and Voltage Lift Switched Inductor (VLSI) are another technique to attain high conversion ratio.

To overcome the above drawbacks a new family called X-Y converter family is proposed by utilizing the feature of Buck-Boost, SI and VLSI. Further, in [14]-[16], X-Y converter family extends to achieve more voltage conversion ratio. But there is less utilization of photovoltaic sources due to discontinuous input current. In [17], DC-DC converter based multistage switched inductor is proposed to achieve a high voltage conversion ratio and continuous input current. But required a large number of inductor and diodes on the input side of the conductor. In [18] modified SEPIC (Single Ended Primary Inductance Converter) are proposed to attain the high voltage conversion ratio by combining the conventional boost and SEPIC. In [19], four configurations of Modified SEPIC with switched inductor are proposed to achieve more voltage conversion ratio as compared to conventional SEPIC. In [20], inverting modified CUK converter is proposed to attain the high voltage conversion ratio.

In this paper a four new configuration of the modified CUK converter is proposed to attain more voltage conversion ratio by combining the feature of switched inductor and modified CUK converter.

Modified CUK Converter with Switched Inductor Configurations (MCC_{SI})

Fig. 1(a) depicts the power circuit of MCC. Fig. 1(b) depicts the circuit of SI module. MCC is derived to attain high conversion ratio by a hybrid combination of boost and CUK converter. Three indictors Lx, Ly and Lz, three capacitors, three diodes and single switch is required to design MCC

The MCC_{SI} configurations are derived by extending the work of modified CUK converter [20]. The MCC_{SI} are classified into four converter configuration (by replacing inductor of MCC by SI. MCC_{SI}-XLL is derived by replacing the Lx inductor of MCC by SI module, MCC_{SI}-LYL is derived by replacing the Ly inductor of MCC by SI module, MCC_{SI}-LLZ is derived by replacing the Lz inductor of MCC by SI module, MCC_{SI}-XYZ is derived by replacing the Lx, Ly and Lz inductors of MCC by three SI module. The power circuits of MCC_{SI}-XLL, MCC_{SI}-LYL, MCC_{SI}-LLZ, MCC_{SI}-XYZ configuration are shown in Fig. 2(a)-(d) respectively. The required number of components to design the proposed configurations for each configuration is provided in Table-I. The working mode with mathematical analysis is discussed in the next section.

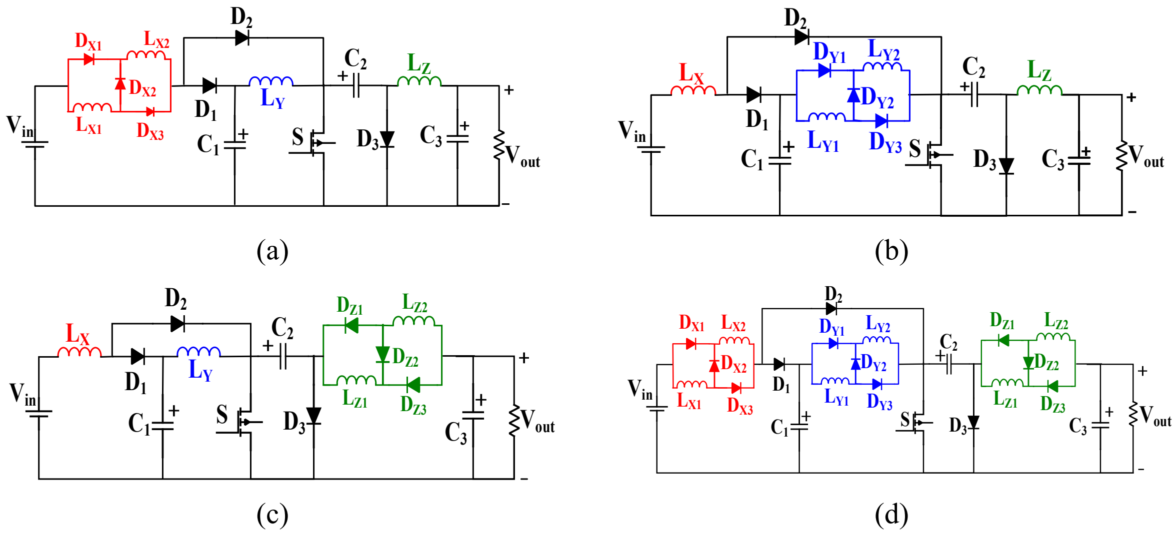

Fig. 2: Different configuration of MCC converter (a) MCC_{SI}-XLL, (b) MCC_{SI}-LYL, (c) MCC_{SI}-LLZ and (d) MCC_{SI}-XYZ

Table I. Number of components and voltage conversion ratio of proposed converter

Modified CUK converter with SI module configuration						
Modified CUK Converter		**Component**			**Voltage Conversion Ratio**	
		L	***C***	***D***	V_{C1}/V_{in}	V_0/V_{in}
SI - Structure	**LLL**	3	3	3	1 / (1-D)	$-D / (1-D)^2$
	XLL	4	3	6	(1+D) / (1-D)	$-D(1+D) / (1-D)^2$
	LYL	4	3	6	1 / (1-D)	$-D(1+D) / (1-D)^2$
	LLZ	4	3	6	1 / (1-D)	$-2D / (1+D)(1-D)^2$
	XYZ	6	3	12	(1+D) / (1-D)	$-2D(1+D) / (1-D)^2$

Working mode of MCC_{SI} Configurations

The working modes of MCC_{SI} is same as MCC, the current flow slightly changes after replacing inductors of MCC by SI module. To boost the voltage, both inductors of SI module are charged in parallel when switch is in conducting state and discharge in series when the switch is not conducting. MCC_{SI}-XLL configuration is considered to explain the operation of MCC_{SI}. It is easy to understand the operation of MCC_{SI}-LYL, LLZ and MCC_{SI}-XYZ after studying the operation of MCC_{SI}-XLL.

When switch of the MCC_{SI}-XLL is conducted, all four inductors L_X (L_{X1} and L_{X2}), L_Y and L_Z are charged from input supply V_{in}, capacitor C_1 and voltage difference of capacitor C_2 and C_3 respectively. The equivalent circuit with characteristic waveforms for the ON-state is shown in Fig. 3(a). In this state, all inductors are charged and capacitors are discharged.

When switch of the MCC_{SI}-XLL configuration is not conducting, inductor L_{X1}, L_{X2} discharged in series with input supply V_{in} to charge capacitor C_1. Inductor L_Y and L_Z are discharged to charge the capacitor C_2 and C_3 respectively. The equivalent circuit with characteristic waveforms for the OFF-state is shown in Fig. 3(b). In this state, all the inductors are discharged and capacitors are charged.

Mathematical Analysis of MCCSI Configurations

This section deals mathematical analysis of MCC, MCC_{SI}-XLL, MCC_{SI}-LYL, MCC_{SI}-LLZ and MCC_{SI}-XYZ configurations. The analysis is done without considering voltage drop across the diode, inductor and one controlled switch (ideal condition). The inductor in each SI module having equal value ($L_{X1}=L_{X2}=L_X$), ($L_{Y1}=L_{Y2}=L_Y$) and ($L_{Z1}=L_{Z2}=L_Z$).

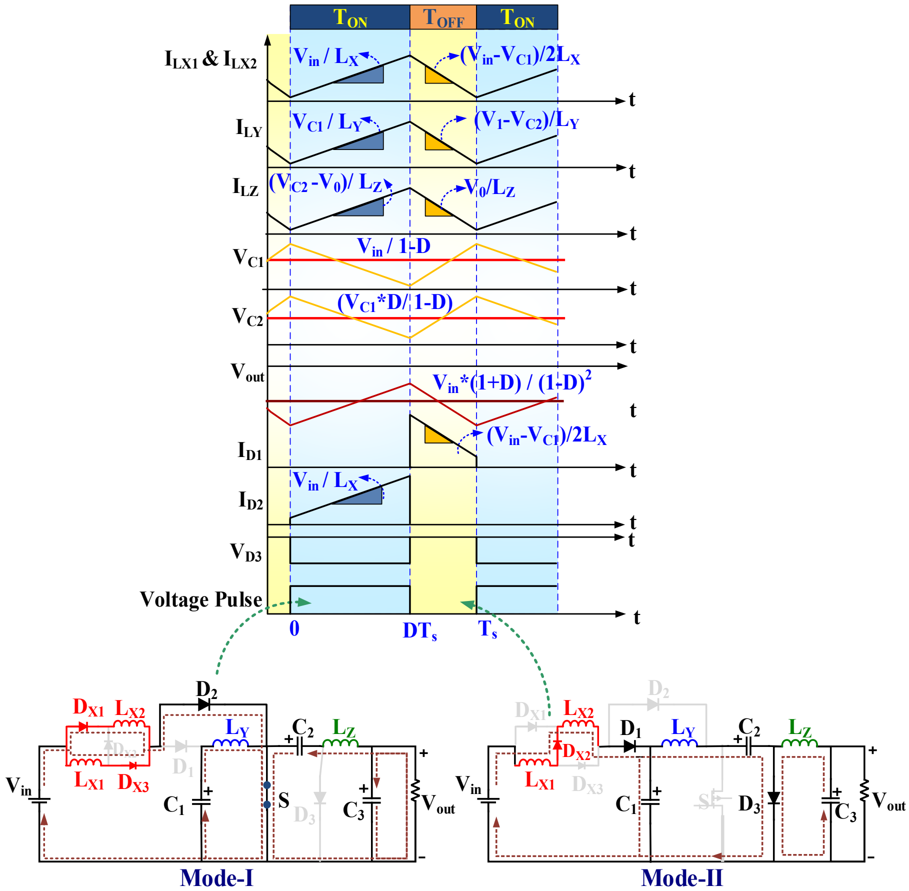

(a) (b)

Fig. 3: MCC_{SI}-XLL working mode (a) charging and (b) discharging

Modified CUK Converter (MCC)

The voltage conversion ratio of MCC-LLL configuration is given in [22]

$$V_0 = \frac{-D}{(1-D)^2} V_{in} \tag{1}$$

MCC_{SI}-XLL Configuration

The equivalent voltage equation of three inductors in ON-state of switch S is

$$\left.\begin{aligned} V_{LX1} &= V_{LX2} = V_{in} \\ V_{LY} &= V_{C1} \\ V_{LZ} &= V_{C3} + V_{C2} \end{aligned}\right\} \text{ON-state} \tag{2}$$

The equivalent voltage equation of three inductors in OFF-state of switch S is

$$\left.\begin{aligned} V_{LX} &= \frac{V_{in} - V_{C1}}{2} \\ V_{LY} &= V_{C1} - V_{C2} \\ V_{LZ} &= V_{C3} \end{aligned}\right\} \text{OFF-state} \tag{3}$$

According to Volt Second Balance Method for inductor L_X, L_Y and L_Z,

$$V_{C1} = \left(\frac{1+D}{1-D}\right)V_{in} \tag{4}$$

$$V_{C2} = \frac{V_{C1}}{1-D} \tag{5}$$

$$V_0 = V_{C3} = -DV_{C2} \tag{6}$$

$$V_0 = -\frac{(1+D)D}{(1-D)^2}V_{in} \tag{7}$$

MCC$_{SI}$-LYL Configuration

The equivalent voltage equation of three inductors in ON-state of switch S is

$$\left.\begin{aligned} V_{LX} &= V_{in} \\ V_{LY1} = V_{LY2} &= V_{C1} \\ V_{LZ} &= V_{C3} + V_{C2} \end{aligned}\right\}\text{ON-state} \tag{8}$$

The equivalent voltage equation of three inductors in OFF-state of switch S is

$$\left.\begin{aligned} V_{LX} &= V_{in} - V_{C1} \\ V_{LY} &= \frac{V_{C1} - V_{C2}}{2} \\ V_{LZ} &= V_{C3} \end{aligned}\right\}\text{OFF-state} \tag{9}$$

According to Volt Second Balance Method for inductor L_X, L_Y and L_Z,

$$V_{C1} = \left(\frac{V_{in}}{1-D}\right) \tag{10}$$

$$V_{C2} = \left(\frac{1+D}{1-D}\right)V_{C1} \tag{11}$$

$$V_0 = V_{C3} = -DV_{C2} \tag{12}$$

$$V_0 = -\frac{(1+D)D}{(1-D)^2}V_{in} \tag{13}$$

MCC$_{SI}$-LLZ Configuration

The equivalent voltage equation of three inductors in ON-state of switch S is

$$\left.\begin{aligned} V_{LX} &= V_{in} \\ V_{LY} &= V_{C1} \\ V_{LZ1} = V_{LZ2} &= V_{C2} + V_{C3} \end{aligned}\right\}\text{ON-state} \tag{14}$$

The equivalent voltage equation of three inductors in OFF-state of switch S is

$$\left.\begin{aligned} V_{LX} &= V_{in} - V_{C1} \\ V_{LY} &= V_{C1} - V_{C2} \\ V_{LZ} &= \frac{V_{C3}}{2} \end{aligned}\right\} \text{OFF-state} \tag{15}$$

According to Volt Second Balance Method for inductor L_X, L_Y and L_Z is

$$V_{C1} = \left(\frac{1}{1-D}\right) V_{in} \tag{16}$$

$$V_{C2} = \left(\frac{1}{1-D}\right) V_{C1} \tag{17}$$

$$V_0 = -\left(\frac{2D}{1+D}\right) V_{C2} \tag{18}$$

$$V_0 = -\frac{2D}{(1-D)^2 (1+D)} V_{in} \tag{19}$$

MCC$_{SI}$-XYZ Configuration

The equivalent voltage equation of three inductors in ON-state of switch S is

$$\left.\begin{aligned} V_{LX1} &= V_{LX2} = V_{in} \\ V_{LY1} &= V_{LY2} = V_{C1} \\ V_{LZ1} &= V_{LZ2} = -V_0 - V_{C2} \end{aligned}\right\} \text{ON-state} \tag{20}$$

The equivalent voltage equation of three inductors in OFF-state of switch S is

$$\left.\begin{aligned} V_{LX} &= \frac{V_{in} - V_{C1}}{2} \\ V_{LY} &= \frac{V_{C1} - V_{C2}}{2} \\ V_{LZ} &= \frac{-V_0}{2} \end{aligned}\right\} \text{OFF-state} \tag{21}$$

According to Volt Second Balance Method for inductor L_X, L_Y and L_Z,

$$V_{C1} = \left(\frac{1+D}{1-D}\right) V_{in} \tag{22}$$

$$V_{C2} = \left(\frac{1+D}{1-D}\right) V_{C1} \tag{23}$$

$$V_0 = -\left(\frac{2D}{1+D}\right) V_{C2} \tag{24}$$

$$V_0 = -\frac{2D(1+D)}{(1-D)^2} V_{in} \tag{25}$$

Simulation Result and Discussion

To verify the functionality, MCC$_{SI}$-XLL, MCC$_{SI}$-LYL, MCC$_{SI}$-LLZ and MCC$_{SI}$-XYZ configurations are simulated in MatLab R2016a. The simulation parameters are provided in Table-II. The controlled

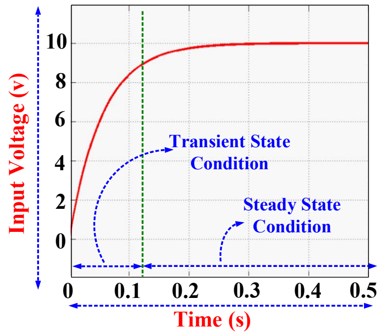

Fig. 4: Controlled input supply

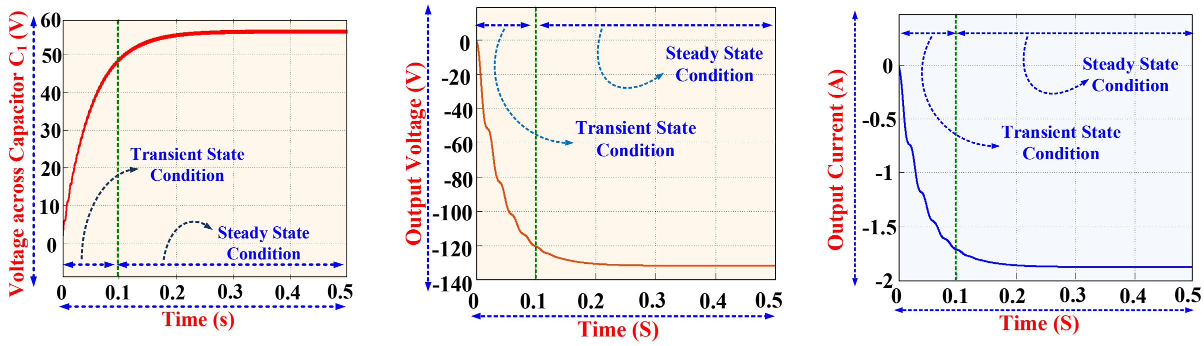

(a) (b) (c)

Fig. 5: Simulation result of MCC$_{SI}$-XLL structure converter (a) Voltage across capacitor C_1, (b) Output voltage, (c) Output current.

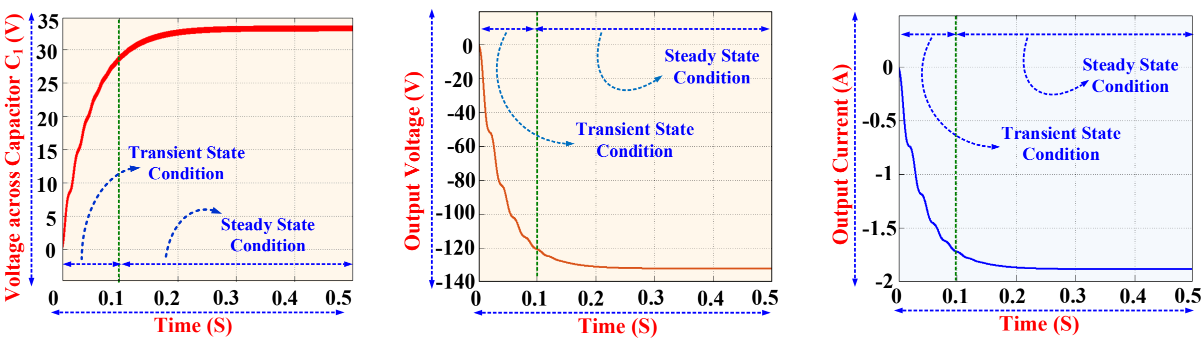

(a) (b) (c)

Fig. 6: Simulation result of MCC$_{SI}$-LYL structure converter (a) Voltage across capacitor C_1, (b) Output voltage, (c) Output current.

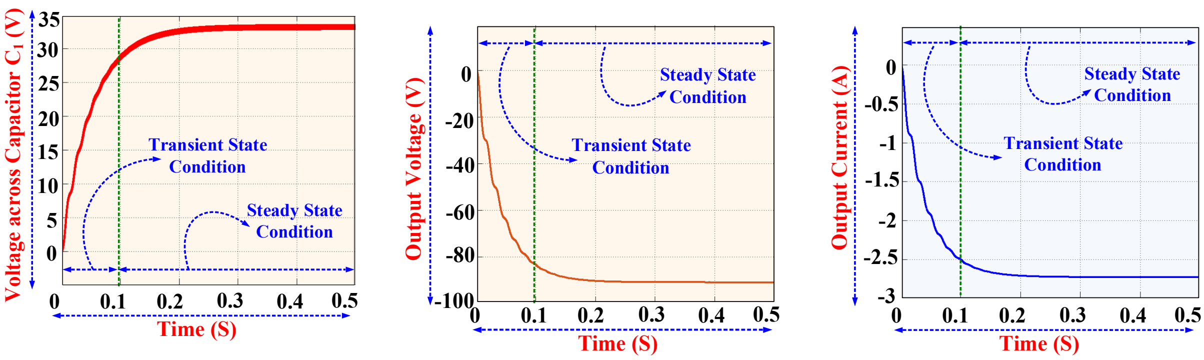

(a) (b) (c)

Fig. 7: Simulation result of MCC$_{SI}$-LLZ structure converter (a) Voltage across capacitor C_1, (b) Output voltage, (c) Output current.

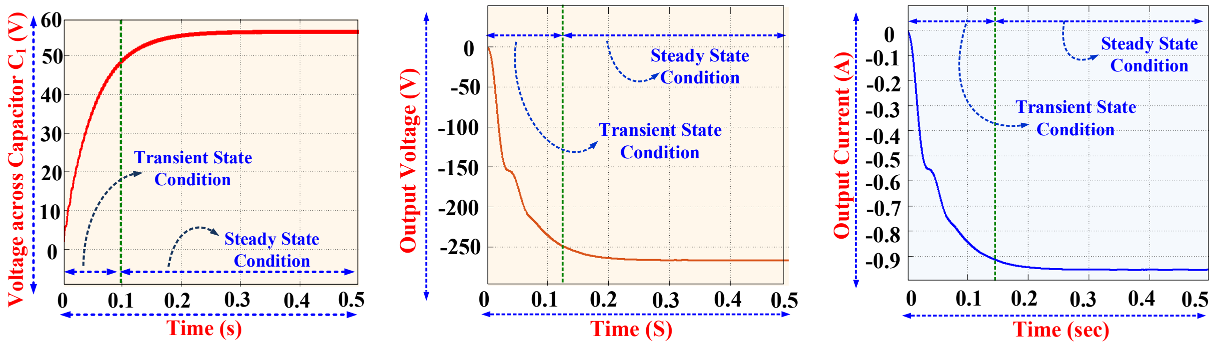

(a) (b) (c)

Fig. 8: Simulation result of MCC_{SI}-XYZ structure converter (a) Voltage across capacitor C_1, (b) Output voltage, (c) Output current.

10V input DC supply is used for simulation with a time constant of 0.05 as presented in Fig.4. The output voltage, output current and voltage across capacitor C_1 is investigated for all the proposed configurations and the obtained results are provided in Table-III.

The voltage across capacitor C_1 of MCC_{SI}-XLL is boosted up to 56.66V as shown in Fig. 5(a). Similarly, the output voltage is boosted to 131.27 V is shown in Fig. 5(b). To meet the power of 250 W, the output current waveform of MCC_{SI}-XLL is shown in Fig. 5(c).

The voltage waveform across capacitor C_1 of MCC_{SI}-LYL is same as the conventional boost converter 33.33 V as shown in Fig. 6(a). The output voltage of MCC_{SI}-LYL is boosted to 131.5 V as shown in Fig. 6(b). The output current waveform of MCC_{SI}-LYL is shown in Fig. 6(c).

The voltage waveform across capacitor C_1 of MCC_{SI}-LLZ is shown in Fig. 7(a). The output voltage waveform of the MCC_{SI}-LLZ is buck up to 116.37 V due to the position of the SI module as shown in Fig. 7(b). The output current waveform of the MCC_{SI}-LLZ is shown in Fig. 7(c).

The voltage across capacitor C_1 of MCC_{SI}-XYZ is boosted to 56.33 V shown in Fig. 8(a). In MCC_{SI}-XYZ configuration, the output voltage is highly boosted up to 263.95 V as shown in Fig. 8(b). The output current waveform of MCC_{SI}-XYZ is shown in Fig. 8(c).

Fig. 9 shows the plot of the voltage conversion ratio versus duty ratio for MCC_{SI}-XLL, MCC_{SI}-LYL, MCC_{SI}-LLZ and MCC_{SI}-XYZ respectively. It is observed that MCC_{SI}-XYZ provides a higher conversion ratio compared to MCC_{SI}-XLL, MCC_{SI}-LYL and MCC_{SI}-LLZ.

Table II. Simulation Parameter

Parameter	Value
Power	250 W
Input voltage	10 V
Duty ratio	70 %
Switching frequency	50 kHz

Table III. Simulation Results of MCC_{SI} family

MCC_{SI} Configuration	Load	Voltage across C_1	Output Voltage	Output Current
MCC_{SI}-XLL	69.75 Ω	56.66 V	131.27 V	1.89 A
MCC_{SI}-LYL	69.75 Ω	33.33 V	131.5 V	1.9 A
MCC_{SI}-LLZ	33.48 Ω	33.33 V	116.37 V	2.13 A
MCC_{SI}-XYZ	279.62 Ω	56.66 V	263.95 V	0.94 A

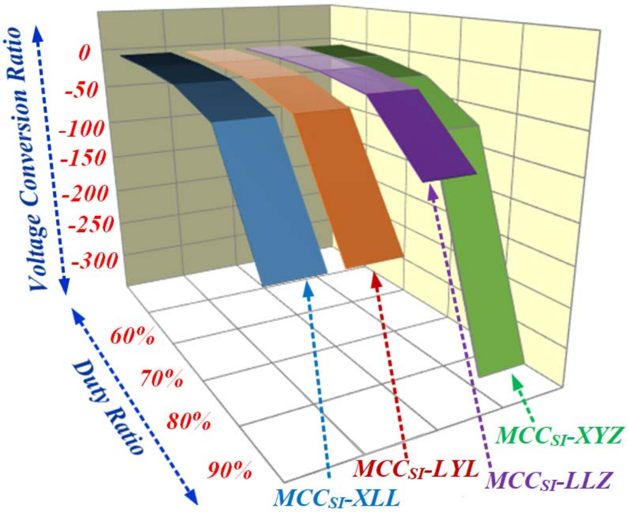

Fig. 9: Voltage conversion ratio VS duty ratio of MCC_{SI} configuration

Conclusion

Four new configurations of MCC with SI module are proposed for high voltage and low current renewable applications. The mathematical equations of voltage conversion ratio for all the configurations are discussed in detail. The comparative analysis of all the proposed configurations with respective to the number of components, voltage conversion ratio is provided. Among the proposed configurations, MCC_{SI}-XYZ configuration provides a higher voltage conversion ratio as compared to MCC_{SI}-XLL, MCC_{SI}-LYL and MCC_{SI}-LLZ. MCC_{SI}-XLL and MCC_{SI}-LYL configurations have low voltage conversion as compared to MCC_{SI}-LLZ and MSC_{SI}-XYZ. The number of components in MCC_{SI}-XYZ is more as compared to other proposed configuration. The simulation results are provided which show a close agreement with theoretical analysis.

References

[1] Sri-Revathi B., Prabhakar M.: Non isolated high gain DC-DC converter topologies for PV applications – A comprehensive review, Renewable and Sustainable Energy Reviews, vol. 66, pp. 920–933, Dec. 2016.

[2] Sanjeevikumar P., Bhaskar M.S., Maroti P. K., Blaabjerg F., Fedák V.: An Original Transformer and Switched-Capacitor (T&SC) Based Extension for DC-DC Boost Converter for High-Voltage/Low-Current Renewable Energy Applications: Hardware Implementation of New T&SC Boost Converter, Energies Journal, MDPI publication Switzerland, 09/2017.

[3] Blaabjerg F., Yang Y., Mam K., Wang X.: Power Electronics-The key Technology for renewable energy system Integration, IEEE-ICRERA'15, 22-25 Nov. 2015.

[4] Forouzesh M., Siwakoti Y, Gorji S., Blaabjerg F., Lehman B.: Step-Up DC–DC Converters: A Comprehensive Review of Voltage-Boosting Techniques, Topologies, and Applications, IEEE Trans. on Power Electronics, vol. 32, no. 12, pp. 9143–9178, Dec. 2017.

[5] Tofoli F. L., Josias de Paula W., D. de S. Oliveira Júnior, D. de C. Pereira: Survey on non-isolated high-voltage step-up dc–dc topologies based on the boost converter, IET Power Electronics, vol. 8, no. 10, pp. 2044–2057, Oct. 2015.

[6] Forouzesh M., Siwakoti Y., Gorji S., Blaabjerg F., Lehman B.: A survey on voltage boosting techniques for step-up DC-DC converters, IEEE-ECCE'16, pp. 1-6, Milwaukee (USA), 18-22 Sept. 2016.

[7] Ismail E., Al-Saffar M., Sabzali A., Fardoun A.: A Family of Single-Switch PWM Converters with High Step-Up Conversion Ratio, IEEE Trans, on Circuits and Systems-I, vol. 55 no. 4 pp. 1159–1171, May 2008.

[8] Sanjeevikumar P., Mahajan S. B., Dhond P., Blaabjerg F., Pecht M.: Non-Isolated Sextuple Output Hybrid Triad Converter Configurations for High Step-Up Renewable Energy Applications, Advances in Power Systems and Energy Management, Lecture Notes in Electrical Engineering, Vol. 436, pp.1-12, Springer Journal Publications, 2018.

[9] Mahajan S. B., Sanjeevikumar P., Pandav K. M., Kulkarni R. M., Sherke V. A.: Buck-Boost Current Converter Using Duality Approach and Its DC Transformer Modeling, Advances in Power Systems and Energy Management, Lecture Notes in Electrical Engineering, Vol. 436, pp.315-324, Springer Journal Publications, 2018.

[10] Tang Y., Fu D., Wang T., Xu Z.: Hybrid switched-inductor converters for high step-up conversion, IEEE Trans. on Industrial Electronics, vol. 62, no. 3, pp. 1480–1490, Mar. 2015.

[11] Chen S., Liang T., Yang L., Chen J.: A Cascaded High Step-Up DC-DC Converter With Single Switch for Microsource Applications, IEEE Trans. on Power Electronics, vol. 26, no. 4, pp. 1146–1153, Apr. 2011.

[12] Rosas-Caro J., Mayo-Maldonado J., Cabrera R., Rodriguez A., Nacu S., Castillo-Ibarra R.: A Family of DC-DC Multiplier Converters, Advance online publication, 10 Feb. 2011.

[13] Bhaskar M. S., Sanjeevikumar P., Blaabjerg F., Fedak V., Cernat M., Kulkarni R. M.: Non isolated and non-inverting Cockcroft-Walton multiplier based hybrid 2Nx interleaved boost converter for renewable energy applications, Conf. Proc, International Power Electronics and Motion Control Conference, IEEE-PEMC'16, pp. 146-151, 25-26 Sept. 2016.

[14] Bhaskar M. S., Sanjeevikumar P., Wheeler P., Blaabjerg F., Rivera M., Kulkarni R.: X-Y converter family: A new breed of buck boost converter for high step-up renewable energy applications, Conf. Proc, International Conference on Automatica, IEEE-ICA-ACCA'16, pp. 1-8, 19-21 Oct. 2016.

[15] MarotiP. K., Sanjeevikumar P., Bhaskar M. S., Blaabjerg F., Fedák, Siano P., Ramachandramurthy V. K.: A Novel 2L-Y DC-DC Converter Topologies for High Conversion Ratio Renewable Application, Conf. Proc, International Conference on energy conversion, IEEE-CENCON'17, 10/2017.

[16] Mahajan S. B., Sanjeevikumar P., Maroti P. K., Fedák V., Blaabjerg F., Ramachandramurthy V. K.: New 2LC-Y DC-DC Converter Topologies for High-Voltage/Low-Current Renewable Applications: New Members of X-Y Converter Family, Conf. Proc, International Conference on Electric Drives and Power Electronics, IEEE-EDPE'17, 4-6 Oct. 2017.

[17] Maroti P. K., Sanjeevikumar P., Bhaskar M. S., Blaabjerg F., RamachandramurthyV. K., Siano P., Fedák V.: Multistage Switched Inductor Boost Converter For Renewable Energy Application, Conf. Proc, International Conference on energy conversion, IEEE-CENCON'17, 10/2017.

[18] Maroti P. K., Bhaskar M. S., Sanjeevikumar P., Blaabjerg F., Fedák V.: A High Gain Modified SEPIC DC-to-DC Boost Converter for Renewable Energy Application, Conf. Proc, International Conference on energy conversion, IEEE-CENCON'17, 10/2017

[19] Maroti P. K., Sanjeevikumar P., Blaabjerg F., Fedák V,, Siano P., RamachandramurthyV. K.: A Novel Switched Inductor Configuration for Modified SEPIC DC-to-DC Converter for Renewable Energy Application, Conf. Proc, International Conference on energy conversion, IEEE-CENCON'17, 10/2017.

[20] Maroti P. K., Sanjeevikumar P., Wheeler P., Blaabjerg F., Rivera M.: Modified High Voltage Conversion Inverting Cuk DC-DC Converter for Renewable Energy Application, IEEE Southern Power Electronic Conference, IEEE-SPEC'17, 12/2017.